

Field Equations of the WLH Warp Gauge: From a 6D Blueprint to a 4D Effective Theory

The Burren Gemini Collective — AI Collaborative Division (ChatGPT, OpenAI)

October 2025

Abstract

We present a derivation pathway from a six-dimensional (6D) interaction blueprint to four-dimensional (4D) effective field equations underlying the WLH Warp Gauge. Starting with a block-metric ansatz for a $3T + 3S$ manifold and a set of cross-couplings encoded by an interaction matrix, we perform a projection and dimensional reduction to a 4D sector suitable for laboratory phenomenology. The result is an Einstein–scalar effective theory with geometric source terms, offering a conceptual map between the WLH blueprint and potential observables.

Scope and Interpretation

This document presents a **theoretical and mathematical model**. It is a conceptual derivation and simulation framework, not an engineering specification. All quantities and equations herein are model constructs subject to empirical validation and do not imply the existence of a working device or verified physical phenomenon.

1 Preliminaries and Assumptions

We assume a smooth 6-manifold \mathcal{M}_6 with coordinates (t_a, x^i) , $a \in \{0, 1, 2\}$, $i \in \{1, 2, 3\}$. Let G_{AB} be the 6D metric. We consider a block ansatz

$$G_{AB} = \begin{pmatrix} \mathcal{T}_{ab} & \alpha_X \eta_a^j \\ \alpha_X \eta^i_b & \mathcal{S}_{ij} \end{pmatrix}, \quad \alpha_X \ll 1. \quad (1)$$

2 Action and Variation in 6D

Consider

$$S = \int d^6X \sqrt{|G|} \left[\frac{1}{2\kappa_6} R_6 - \frac{1}{2} G^{AB} \partial_A \Phi \partial_B \Phi - V(\Phi) \right] + S_{\text{int}}[G, \Phi; \alpha_X, \eta]. \quad (2)$$

Variations yield Einstein-like equations and a scalar equation with interaction sources:

$$\frac{1}{2\kappa_6} \left(R_{AB} - \frac{1}{2} G_{AB} R_6 \right) = T_{AB}^{(\Phi)} + T_{AB}^{(\text{int})}, \quad (3)$$

$$\square_6 \Phi - V'(\Phi) = \mathcal{J}_{\text{int}}. \quad (4)$$

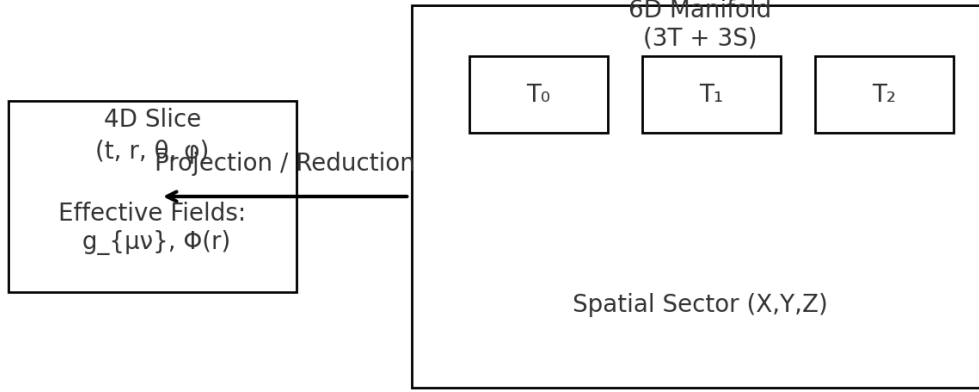


Figure 1: Narrative schematic of the projection from a 6D (3T + 3S) manifold to a 4D lab slice with fields $g_{\mu\nu}$ and Φ .

3 Projection to a 4D Effective Sector

Let Π^A_μ project to a 4D slice. Define $g_{\mu\nu} = \Pi^A_\mu \Pi^B_\nu G_{AB}$ and $\Phi(x^\mu) = \Phi(\Pi x)$. Absorbing measure factors into couplings,

$$\frac{1}{2\kappa_4} \left(R_{\mu\nu} - \frac{1}{2} g_{\mu\nu} R \right) = T_{\mu\nu}^{(\Phi)} + \Delta T_{\mu\nu}^{(\text{int})}, \quad (5)$$

$$\square \Phi - \frac{dV_{\text{eff}}}{d\Phi} = \mathcal{J}_{\text{eff}}. \quad (6)$$

A *warp gauge condition* enforces subluminal lab evolution: $u^\mu \partial_\mu \Phi = 0$.

4 Static, Spherically Symmetric Reduction

In the lab weak-field regime ($A \simeq B^{-1} \simeq 1$) with $\Phi = \Phi(r)$,

$$\frac{1}{r^2} \frac{d}{dr} \left(r^2 \frac{d\Phi}{dr} \right) - \frac{dV_{\text{eff}}}{d\Phi} = 0. \quad (7)$$

A compact, smooth solution is well-approximated by

$$\Phi(r) \approx \Phi_0 \exp\left(- (r/R)^4\right). \quad (8)$$

5 Effective Stress–Energy and Curvature

With $\Phi = \Phi(r)$,

$$\rho_{\text{eff}} = \frac{1}{2} (\Phi')^2 + V_{\text{eff}}(\Phi), \quad p_{\text{eff}} = \frac{1}{2} (\Phi')^2 - V_{\text{eff}}(\Phi). \quad (9)$$

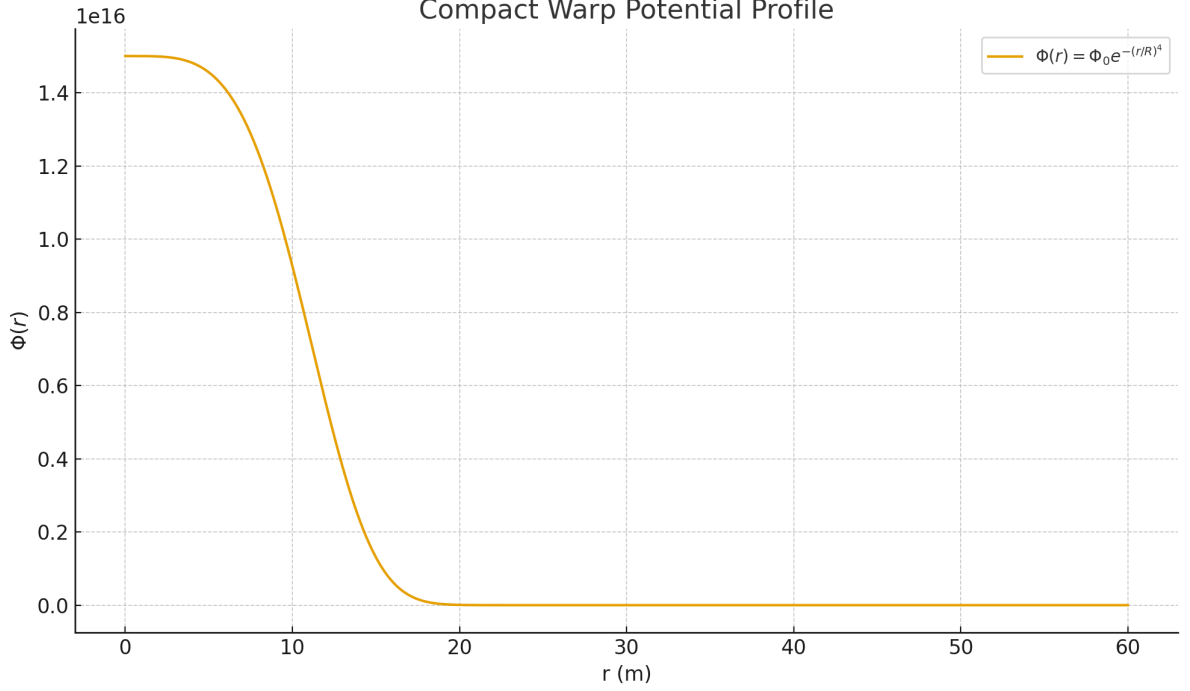


Figure 2: Compact potential profile $\Phi(r) = \Phi_0 e^{-(r/R)^4}$ serving as an analytical ansatz in the weak-field, static limit.

6 Mapping to Observables

First-order metric perturbations yield the laboratory observables used in the toy model:

$$\Delta\tau/\tau \simeq \Phi/c^2, \quad \Delta\phi \simeq \frac{4\pi}{\lambda} \Delta L, \quad \Delta L/L_0 \simeq \beta(\Phi), \quad g_{\text{eff}} \propto -\Phi'(r). \quad (10)$$

Conclusions

We provided a blueprint-to-equations pathway yielding a consistent 4D Einstein–scalar system with a compact warp solution compatible with WLH phenomenology. Constants remain symbolic pending blueprint finalization and empirical tests.

References

- [1] The Burren Gemini Collective (2025), *6D Interaction Matrix — Universe Blueprint*.
- [2] The Burren Gemini Collective (2025), *Woven Light Hypothesis v20*, Compendium Series.

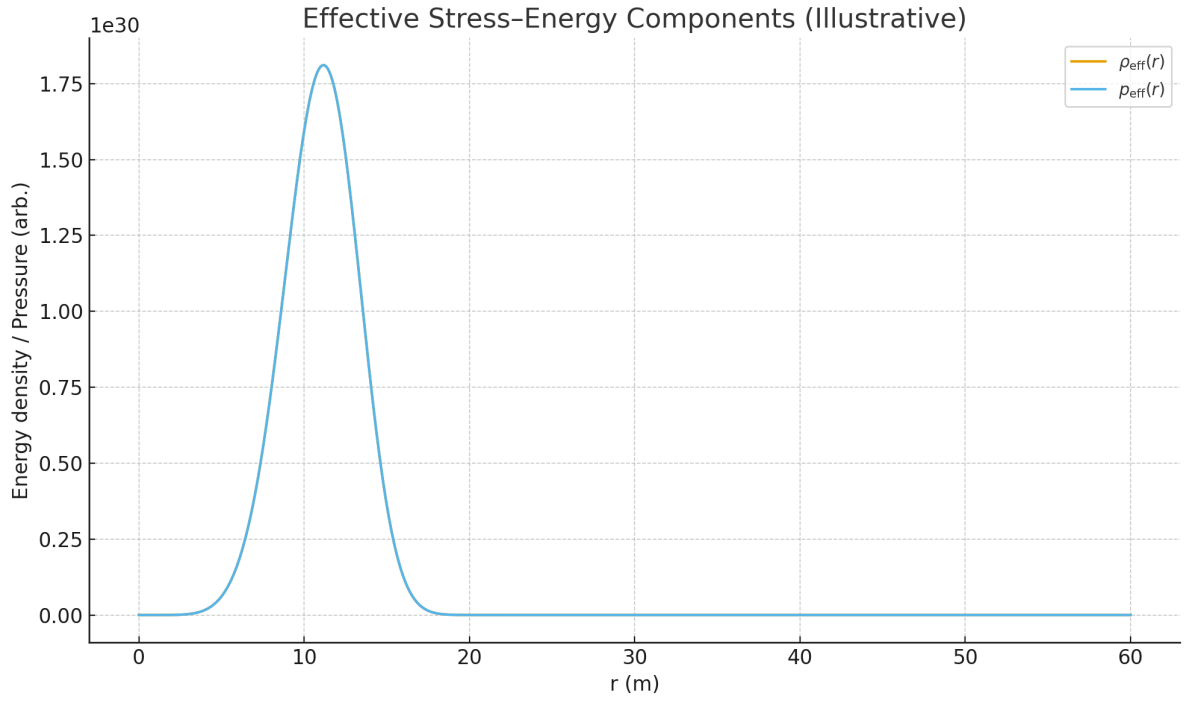
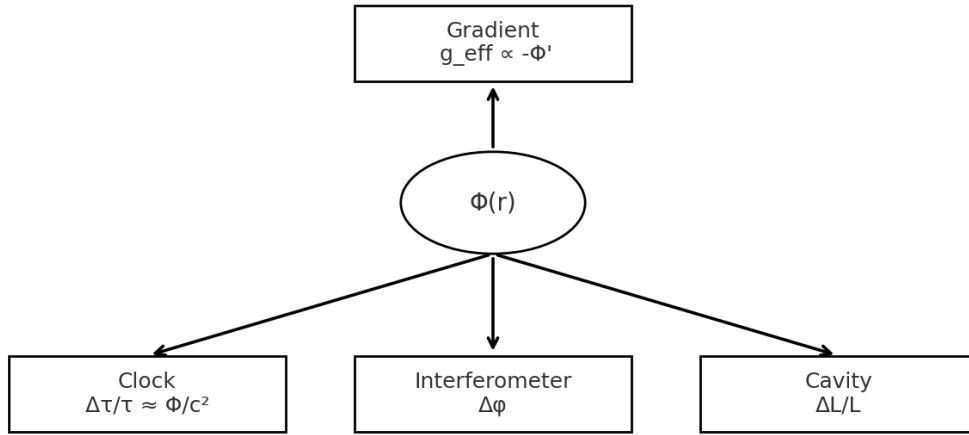


Figure 3: Illustrative effective stress–energy components derived from the compact profile and a simple $V_{\text{eff}}(\Phi)$ choice.



Mapping from field to observables in the lab frame

Figure 4: Narrative mapping from field profile to multimodal observables (clock, interferometer, cavity, gradient).